Beverly Clark III, Gamil Gurguis and H.D. Hallen, "Nanoscale optical imaging of pigment particles in paint with near-field scanning optical microscopy," Journal of Vacuum Science and Technology B: Microelectronics and Nanometer Structures 25, 54 - 57, 2007.

Nanoscale Optical Imaging of Pigment Particles in Paint with Near-field Scanning Optical Microscopy

Beverly Clark III[†], Gamil Guirgis*, H.D. Hallen[†]

[†]Department of Physics, North Carolina State University, Raleigh North Carolina 27695

*Department of Chemistry & Biochemistry, College of Charleston, Charleston SC 29424

ABSTRACT

The distribution of pigment at the nano- to micron scale illuminates the length-scale of failure in paint samples. We use optical and topographical images from Near-field Scanning Optical Microscopy (NSOM) to compare a high quality paint sample with one that fails a standard quality control test based upon visual inspection. NSOM provides the required nanometer to micrometer mesoscopic regime resolution and range, combined with simultaneous topographic and optical information. Features such as pigment clumping and pigment density fluctuations are simultaneously analyzed. The two types of samples are distinguished by fluctuations at different length scales. We observe individual pigment particles near the polymer surface of both samples.

1. INTRODUCTION

Paints are industrially important materials. To provide a uniform surface coating, quality control requires detection of the defect and corrective action requires knowledge of the cause. This project defines a set of mesoscopic, measured criteria that can be used in a quantitative manner to identify the quality of paint samples. The criteria are qualitative: the paint must look 'good' to the human eye, meaning uniform, deep color. The translation of this into a machine-measured quantity is not obvious, but was assumed to be in the mesoscopic regime, since the material must be non-uniform at some regime given the quantized size of pigment particles. To identify the defects, we investigate the nanometer to micrometer (mesoscale) regime with optical and topographical surface characterization. In particular, a unique approach is presented for identifying and characterizing surface features through the use of near-field scanning optical microscopy (NSOM).

NSOM enables simultaneous, high-resolution optical and topographical imaging of mesoscale surface features [1, 2]. Light is input through a chemically etched and metal coated fiber optic probe [3]. The probe is brought within nanometers of a sample surface and rastered while the topographical and optical signal are simultaneously collected [4, 5]. The statistical analysis of these observations characterizes surface features such as clumping, pigment density fluctuations, and overall smoothness of sample surfaces.

Although the use of mesoscopic traits to distinguish paint quality is not surprising, the form it takes is unexpected. The statistical analysis of the length scale of both optical and topographic features provides a good characteristic that distinguishes paint quality. Surprisingly, there is a peak in this distribution at nonzero length scale for the good paint, whereas the poor quality paint's distribution decreases more or less uniformly with length scale. Presumably, variation at a small length scale satisfies the requirement of variation at some length scale, while the variation at small, mesoscopic length scales both is not resolved by the eye and adds the sensation of a 'deep' color. This technique can be useful for focusing on material design and correcting material design. In the process, we found that individual pigment particles can be identified. Many individual data sets were imaged and defined as follows: from a reference sample, R, of high quality or from a low quality sample, N. The quality value is based upon visual inspection. This study of the samples shows that quality variations are differentiated at the mesoscopic length scales over which both the optical and topographic signals vary. The length scale of the fluctuations is more important for observing paint quality than the actual fluctuations.

2. METHODS

NSOM allows the corroboration between topographic and optical signals as it enables the extension of optical techniques for higher resolution imaging [5, 6]. Although other methodologies can be used, NSOM is a straight-forward method; light can be 'focused' on the region of interest easily and efficiently. In order to obtain high-resolution images, the system must be free of vibrational noise, the tip must be close to the sample, and stable feedback must be established [2]. Spatial Resolutions of the topographic signal is determined by the radius of curvature of the end of tip, which is ≈ 10nm. The optical

signal is determined by the size of the tip aperture and some contribution due to distance away from sample [3, 7]. We can measure them by measuring the full width at half maximum of a feature that is small compared to the resolution. The individual pigment particles provide a feature on the order of the resolution size, and can be used to set an upper limit on the optical resolution for this work [7], ~25 nm.

In our system, shear-force feedback is the method of probe sample distance control [7, 8]. The NSOM setup uses a tuning fork oscillator to detect the tip oscillation amplitude and control the separation of the tip and sample [6]. Shear force feedback uses voltage generation by a quartz crystal tuning fork to measure the oscillation amplitude that varies with distance [7, 8]. Fiber probes (etched and metal coated) are rigidly mounted with superglue to the side of the tuning fork [9]. The tuning fork's resonance frequency is altered by the presence of the mounted probe [4]. The frequency changes from ~33 kHz to ~40 kHz due to stiffening of the mechanical oscillator (tuning fork and fiber). Once the probe is close to the sample surface, there is a change in resonance frequency and the oscillation amplitude decreases[1]. The nonlinear tapping interaction between the probe and layers adsorbed on the sample is used to increase the operational bandwidth of this high quality factor oscillation system [7].

To identify pigment distributions and individual particles, topographical and optical data were collected. For collection of topographical information, the optical probe raster scans across the specified scan range under z feedback collecting forward and backward data (in both directions) on the contour of the sample [6, 10]. The forward and backward images

are correlated to insure artifact-free imaging and to determine noise levels [11]. For collection of optical data, a collection lens relays reflected light into a photomultiplier tube (PMT). Both the PMT and collection lens are located at a 45 degree angle to the sample surface normal. HeNe laser light (**6**32.8nm) coupled into the optical probe is used for sample illumination. Both forward and backward optical images are accumulated and analyzed.

3. RESULTS AND DISCUSSION

Several areas on each of the reference and low quality samples were imaged and compared. The topographic images required background subtraction, calculated from a least squares fit of a plane to a sub region of the image. It corrects for an overall tilt of the sample. The quality of these otherwise unprocessed images is remarkable given the nature of the sample (the topography is microns in height over microns in lateral motion). On such samples, tip switching will occur when a groove is too narrow for the probe to fit into, and causes imaging to begin with a different part of the probe. It is observed [12, 13] in some of the images here, such as near the top of Fig. 3. Such expected effects are not a cause for concern if they are reproducible, as they are here. Data near the tip switch must be analyzed with the probe shape in mind.

This paint sample is largely clear polymer, with opaque (at some wavelengths) pigment particles imbedded in it. The pigment particles are small enough to cause significant scattering, and scattering from the pigment particles is the source of most of the signal from these particles viewed with NSOM [11, 13]. A clear sample usually does not show

significant topographic-induced artifacts in the optical image due to the nonlinear influence of the probe boundary conditions on the optical coupling. Such artifacts are usually due to narrow topographic features or poor distance regulation, so occur at edges. When variations continue well beyond edges, they are likely not artifacts [11, 13]. Multiple images of 'forward' and 'backward' data for a particular image were analyzed and compared to distinguish between artifacts and actual structures. Distance-regulation related artifacts will be different in the forward and backward data, but real features will repeat[12, 13]. We only observe topographic-induced artifacts in the optical images near lines of tip switching in the data presented here. In analyzing forward and backward line cuts, the anticipated hysteresis (due to inherent losses in the piezo-tube scanner during large scans [14]) is visible as a lateral shift, ~100 nm here, between the images.

Figures 1 and 2 are images of the reference sample. Aligned, uniform circular structures can be seen, as expected from the reference sample. In Figure 2, it is possible to see the ridging of the polymer in the lower right corner of the image. The image scale ranges from white (highest point value) to black (lowest point value) over a scan range of 1.92 microns, which is also the scan range for Figure 1. Similarities in the optical and topographical images indicate a coupling between topography and pigment distribution. Due to the large size scale and comparison of forward and backward images, we know that this is not a NSOM 'topographical artifact' but rather a real coupling between pigment density and topography [12, 15].

Low quality sample images show pigment particles in non-uniform arrangements, and particle clumping was often observed as shown in Figure 3. This 3.2 micron square image is a little more than 1 ½ times larger than that of the reference sample, and the height range is similarly larger. The optical data look qualitatively similar between Figure 2 and Figure 3(b), but the optical scale in Figure 3(b), the lower quality sample data, is about 5 times larger than that of the reference sample, so there is in fact a much larger variation in optical signal. Some of these variations are coupled to the topography, and some seem not to be correlated, instead representing clumping of the pigment particles.

Knowing that we have a resolution (with both light and topography) near that of the pigment particle size and can identify what we believe to be the polymer structure, we focus on discriminating between the reference and low quality sample. We recorded and plotted the long and short-term height variations in the two paint samples. Short-term variations are defined as variations over a 300-500 nm length scale (up to one quarter the image size), and long-term variations are defined as variations over the interval of the entire image range (1-2 μm). Overall, 62 images (optical and topographical) were evaluated for long and short-term variations. For each long and short scale variation, two numbers were recorded; the first is the variation defined above and the second is the maximum value in the image. Each number was the average of three measurements of the same variation. The percent variations were obtained by dividing the first number by the second and multiplying by 100. The reason for normalization is to correct for variations of laser power or probe through-put in various images. The throughput is highly probe-dependent, and normalization allows quantitative comparisons of data from different

probes (given that the resolution of the probes is better than the feature size of interest, easily true here). These ratios (long and short scale) were plotted and used to analyze the two paint samples.

From the histograms (Figure 4), we note the optical Reference, R, data are strongly peaked at low percent variation for both long and short-term variations, whereas the low quality samples, N, show a much wider range in variation on all length scales ranging from very small variations (peaking near zero) to large variations (beyond the peak of R). That is, the Reference data are strongly peaked at a nonzero (but small) variation, and drop sharply to zero, whereas the low quality samples decrease from a maximum near zero and exhibit a much longer tail. These mesoscopic traits distinguish the two paint samples.

SINGLE PIGMENT PARTICLE IMAGING

Individual pigment particles were identified in several scans. Evidence of these single particles can be found in an image by expanding small regions of the images and scaling the color table, but is much more convincing in the forward and backward line cut data. The line cut data allows us to look at z versus x or y, all measured in nanometers. It is free from color-table induced artifacts and elucidates the noise levels. Correlations of peaks in the forward and backward data of the optical and topographical scans corroborate identification of single pigment particles. The particles identified were 20-30 nm in 'half-height' diameter, which is approximately our optical resolution. Figure 5 shows the optical data in which arrows indicate the individual pigment particles, shifted

between the forward and backward data by hysteresis. The same particles were verified in the topographical data.

4. CONCLUSIONS

Pigment particles near the sample surface were imaged with NSOM. Images of polymers in the paint sample also identified large scale structures such as polymer ridges and clumped pigment. The scans of the low quality sample showed non-uniform arrangements of pigment particles and also non-uniform particle clumping. Statistical analysis of paint sample images yields information about the mesoscale order of the pigment distributions. The histograms (Figure 4) illustrate our approach using the long and short term variations to distinguish between the low and high quality samples. The NSOM approach for sample identification and characterization was effective in allowing us to resolve features in the mesoscale regime, which distinguish high and low quality paints in a manner that can be implemented on a machine rather than 'by eye,' and point to the qualities of a good paint.

ACKNOWLEDGEMENTS

This material is based upon work supported by the National Science Foundation under grant numbers DMR-9975543 and DMII-0210058. This research was also sustained by fellowship support from the U.S. Department of Education Graduate Assistance in Areas of National Need (GAANN) Fellowship Program (P200A000854).

LITERATURE CITED

1. C.L. Jahncke and H. D. Hallen, J. Appl. Phys. **93**, 1274 (2003).

2. E. Betzig and J. Trautman, Science **257**, 189 (1992).

3. A. Lazerev, N. Fang, Q. Luo, and X. Zhang, Rev. of Sci. Instrum. **74**, 3679 (2003).

4. K. Karrai and R. Grober, Proceedings of SPIE, edited by Michael A. Paesler and Patrick J. Moyer 2535, 69 (1995).

5. R. Brunner, A. Bietsch, O. Hollricher, O. Marti, Rev. Sci. Instrum. **68**, 1769 (1997).

6. J. Hsu, Mat. Sci. Engin. **33**, 1 (2001).

7. C.L. Jahncke, S.H. Huerth, Beverly Clark III, and H.D. Hallen, Appl. Phys. Lett. **81**, 4055 (2002).

8. K. Karrai and R. Grober, Appl. Phys. Lett. **66**, 1842 (1995).

9. D. Davydov, K. Shelimov, T. Haslett, M Moskovits, Appl. Phys. Lett **76**, 1796 (1999).

10. M. A. Paesler, P.J. Moyer, Near-field Optics: Theory, Instrumentation, and Applications, Wiley & Sons (1996).

11. O. Fenwick, G. Latini, F. Cacialli, Synthetic Materials **147**, 171 (2004).

12. S. Bozhevolnyi, J. Opt. Soc. Amer. B **14**, 2254 (1997).

13. X. Wang, Z. Fan, T. Tang, J. Opt. Soc. Amer. A **22**, 2730 (2005).

14. D. Croft, G. Shed, S. Devasia, J. of Dyn. Syst., Meas., and Contr.**123**, 35 (2001).

15. B. Hect, H. Bielefeldt, Y. Inouye, D. Pohl, J. Appl. Phys. **81**, 2498 (1997).

1.

Beverly Clark III
Journal of Vacuum Science and Technology (B)

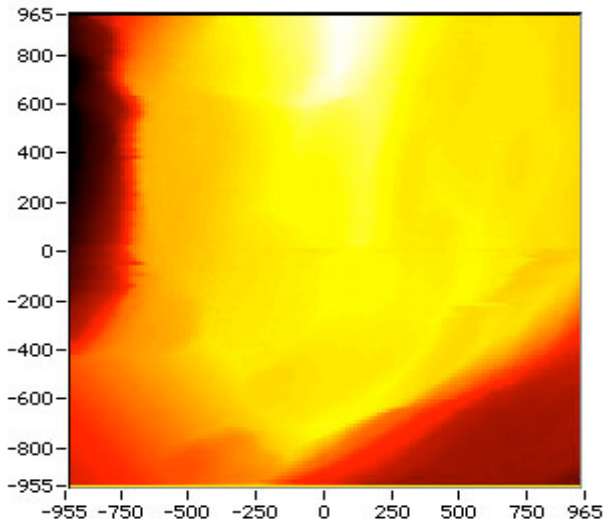

Figure 1: This is a topographic scan of the reference sample (1905 nm x 1905 nm). The axes are in nanometers. The overall z distance range is 1360 nm. The middle region of the image represents one plateau at a vertical position near 228 nm. The upper middle portion of the image is 225 nm above the middle plateau, and the bottom right where polymer ridging is observed is 800 nm below the middle plateau.

2.

Beverly Clark III

Journal of Vacuum Science and Technology (B)

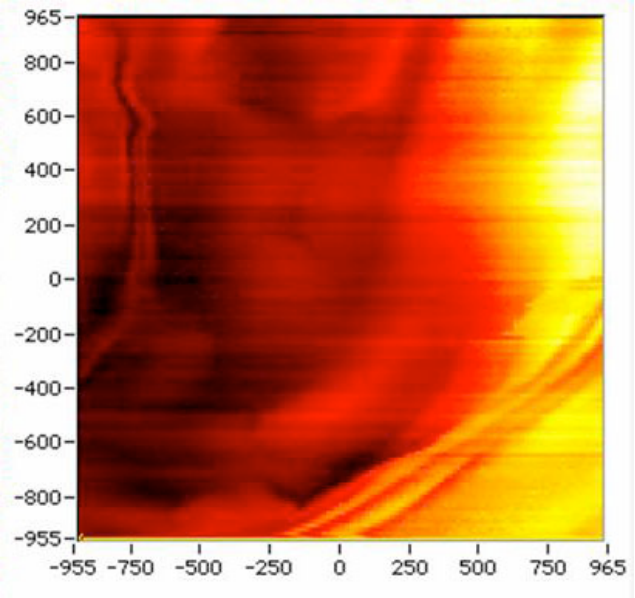

Figure 2: This is an optical scan of the reference sample (1905 nm x 1905 nm). The optical range was measured in arbitrary units. The horizontal axis is in nanometers. There is an overall optical range of 0.051 a.u. In the upper left and lower right portions of the image, polymer ridging is observed. This is consistent with Figure 1, which was taken over the same scan range.

3. Beverly Clark III, Journal of Vacuum Science and Technology (B)

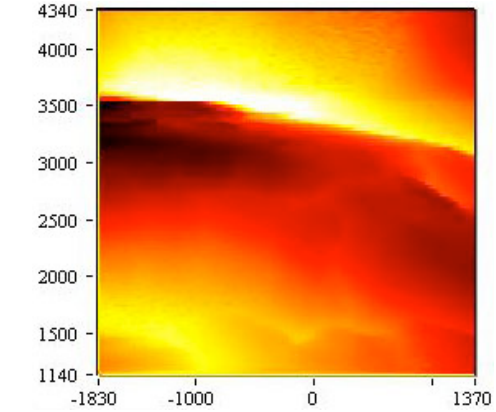

(A)

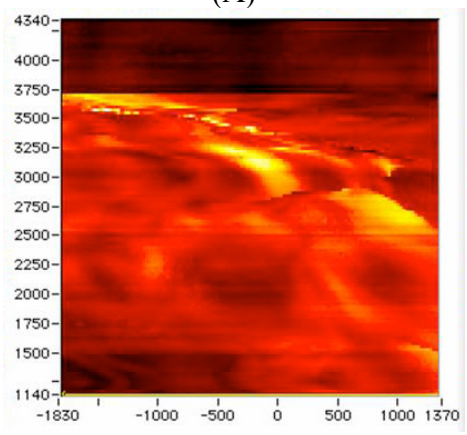

(B)

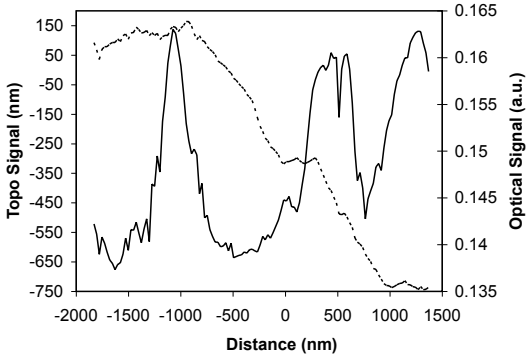

(C)

Figure 3: (A) and (B) are topographic and optical images of the low quality sample, respectively. Both scans are (3200 nm x 3200 nm), and were simultaneously acquired. The overall topographic range is 1895 nm and the optical range of 0.27a.u. The scans show pigment particle clumping in a non-uniform manner. (C) Horizontal line-cuts taken from 1/3 the way up (A) and (B). The dashed line represents the topographical signal and the solid line represents the optical signal.

4.

Beverly Clark III
Journal of Vacuum Science and Technology (B)

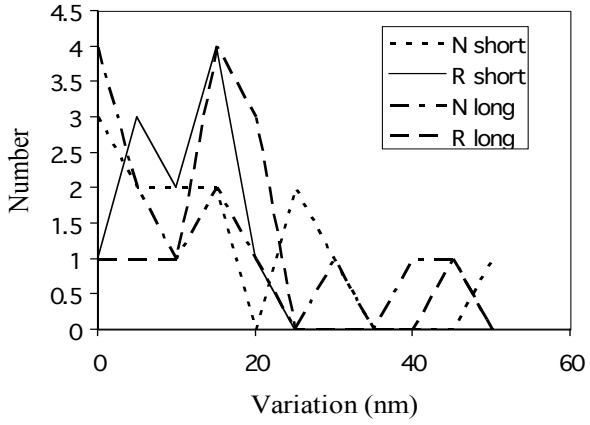

(A)

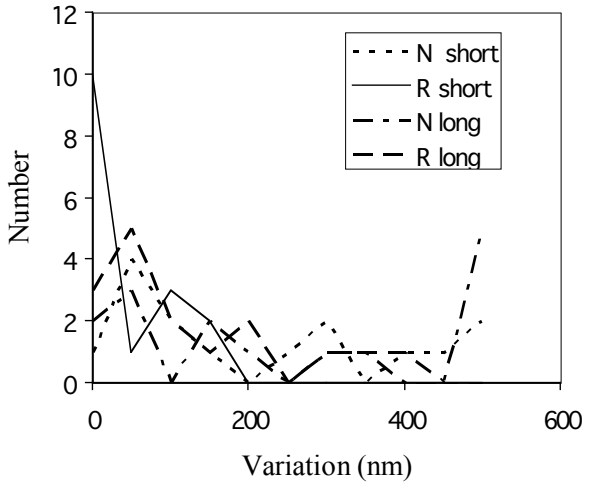

(B)

Figure 4: (A) is a histogram of the optical variation and (B) a histogram of the topographical variation. In analyzing the percent variation, it is possible to distinguish between the reference and low quality sample.

5.

Beverly Clark III
Journal of Vacuum Science and Technology (B)

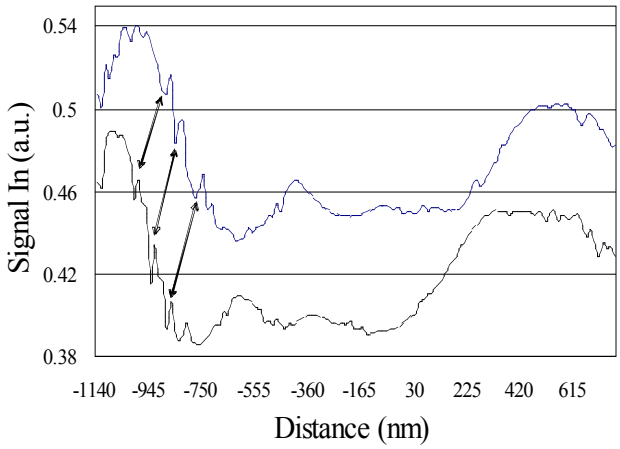

Figure 5: This is the optical forward/backward line-cut data from the lower portion of Figure 3. The forward data have been shifted upward for clarity. The horizontal axis is distance (nm), and the vertical axis is in arbitrary units. The forward data (top graph) is shifted to the right of the back data (bottom graph) due to hysteresis. The arrows indicate corresponding data points in the forward and backward data that reflect the same pigment particles.